Nuclear Magnetic Resonance Determination of Intramolecular Distances in Bovine Pancreatic Trypsin Inhibitor Using Nitrotyrosine Chelation of Lanthanides†

Timothy D. Marinetti,‡ Grayson H. Snyder,§ and Brian D. Sykes*

ABSTRACT: Nitration of tyrosine has been investigated as a means for chemically introducing lanthanide chelating sites at known positions in proteins. The low-field portions of the 250-MHz and 270-MHz ^{1}H nuclear magnetic resonance spectra of native and chemically modified bovine pancreatic trypsin inhibitor have been studied in the presence of lanthanide ions. Comparisons of spectral changes observed with native, mononitro (tyrosine 10) and dinitro (tyrosines 10 and 21) derivatives enable these changes to be separately attributed to metal bound at nitrotyrosine 21, nitrotyrosine 10, or the set of five carboxyl groups. The pH dependence of Pr(III) and Eu(III) induced chemical shifts yields stability constants of 50 and 159 M^{-1} for the association between lanthanides and nitrotyrosines 10 and 21, respectively. Correlation times for the interactions with Gd(III) bound to specific nitrotyrosines are estimated from the induced line broadening of resonances of the nitrotyrosine ring protons. These stability constants and correlation times are used to determine the distances from the different metal binding sites to buried backbone NH protons having resolved resonances. Comparisons with distances in the x-ray crystal structure give assignments of the NH resonances to a small set of buried backbone NH's.

Lanthanide ions have been used extensively in recent years as probes of molecular structure by observing the specific shift and relaxation effects they induce in the nuclear magnetic resonance spectra of their complexes (LaMar et al., 1973; Reuben, 1973; Sievers, 1973). Many biological applications of these metals have been recently reviewed (Reuben, 1975). Specific examples include structural studies of nucleotides (Barry et al., 1972, 1974a,b; Dobson et al., 1974) and the enzyme lysozyme (Campbell et al., 1973, 1975; Jones et al., 1974) and studies of substrates bound to a lysozyme–lanthanide complex (Butchard et al., 1972).

A requirement for the use of these metals is that the molecule under study possesses a specific binding site at a known locus in the structure. In lysozyme, two spatially adjacent carboxyl side chains, aspartate 52 and glutamate 35, form a strong binding site (Morallee et al., 1970; Butchard et al., 1972). However, not all proteins possess such a naturally occurring site; even if one were present, its position would not be known unless crystallographic information was available. In such cases, introduction of a chelating function by chemical modification at a known location might facilitate the use of lanthanide ion probes (Campbell et al., 1973). Selective nitration of tyrosines has been proposed as such a modification (Marinetti et al., 1975). Specific nitration of tyrosines in proteins has been reported in a wide variety of systems (Riordan and Sokolovsky, 1971; Riordan and Vallee, 1972), so this chelator has potential applicability to many proteins. The successful use of nitrotyrosine as a specific lanthanide chelator in a protein is reported below in experiments with the bovine basic pancreatic trypsin inhibitor.

BPTI[1] is a small protein with a known x-ray structure (Diesenhofer and Steigemann, 1974; Huber et al., 1974), known procedures for nitration (Meloun et al., 1968), and stability over a wide pH range (Vincent et al., 1971). The ring proton resonances of the tyrosines and nitrotyrosines in BPTI and its nitrated derivatives have been located and assigned to specific positions of specific rings (Snyder et al., 1975). The protein's small size leads to relatively narrow lines, and the spectrum shows many resolved resonances, including at least nine resonances of area one associated with individual buried backbone NH protons (Karplus et al., 1973; Masson and Wüthrich, 1973). This facilitates observation of the effects of lanthanides bound to the chelating groups of the molecule, e.g., shifts with Pr(III) and Eu(III) and line broadening with Gd(III). In this manuscript, the interactions of these metals with the nitrotyrosines of nitrated BPTI derivatives are studied. By comparison of spectral changes observed with different derivatives, these changes can be separately attributed to metal bound at nitrotyrosine 21, nitrotyrosine 10, or the set of five carboxyl groups. Stability constants obtained from the observed pH dependence were used to quantitatively interpret the Gd(III) induced line broadening of the resolved NH resonances to obtain distances to the different metal binding sites. Five of these NH protons are very close to tyrosine 21. This fact indicates that the polypeptide chain at the base of the molecule is sufficiently rigid to prevent exchange of intramolecularly hydrogen bonded NH protons on the timescale of several months. By comparing the NMR distances with those calculated from the crystal structure, these NH's were assigned to a set of backbone positions.

Materials and Methods

BPTI was obtained as a gift from Farbenfabriken Bayer AG

From the Department of Biochemistry and the Medical Research Council Group on Protein Structure and Function, University of Alberta, Edmonton, Alberta, T6G 2H7, Canada. *Received April 16, 1976.* This work was supported in part by the National Institutes of Health (Grants GM-17190 and RR-00292 (NMR Facility for Biomedical Studies)) and the Medical Research Council of Canada Group on Protein Structure and Function. This paper taken in part from the Ph.D. thesis of T.D.M., Harvard University, 1975.

‡ Present address: Department of Physics, University of California, San Diego, La Jolla, Calif. 92093.

§ Present address: Department of Biochemistry, Stanford University School of Medicine, Stanford, Calif. 94305.

[1] Abbreviations used: BPTI, basic pancreatic trypsin inhibitor; Pipes, piperazine-*N*,*N*′-bis(2-ethanesulfonic acid); DSS, 2,2-dimethyl-2-silapentane-5-sulfonic acid; HMDS, hexamethyldisiloxane.

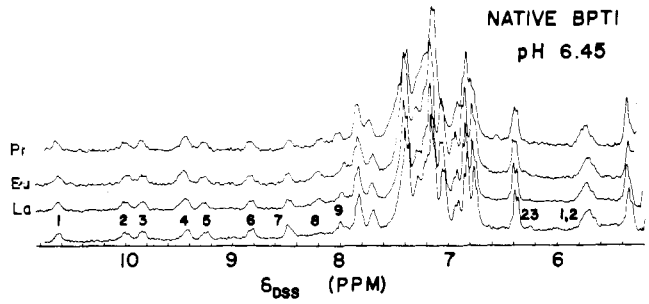

FIGURE 1: Low-field portion of the 250-MHz NMR spectrum of native BPTI at pH 6.45 with various metals. Buffer is 15 mM Pipes, 0.5 mM DSS, and 0.1 M KCl in D_2O. [BPTI] = 2.4–2.5 mM. In the upper three spectra containing one lanthanide apiece, [La(III)] = 17.1 mM, [Eu(III)] = 17.8 mM, and [Pr(III)] = 17.8 mM. The lower trace is the spectrum in the absence of metal ions. Spectra are the sum of 1000 rapid scans using correlation spectroscopy. Sweep width is 2900 Hz, digitized in a scan of about 1.5 s. See Materials and Methods for details.

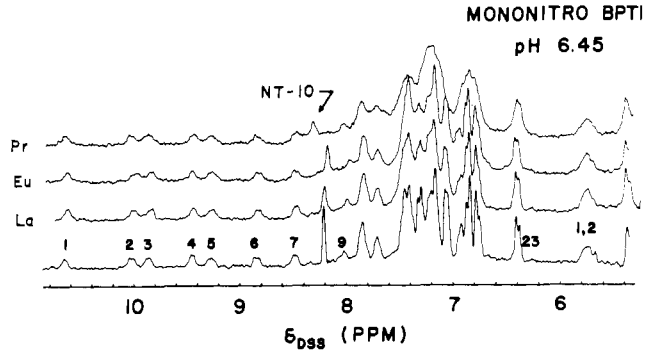

FIGURE 2: Low-field portion of the 250-MHz NMR spectrum of mononitrated BPTI (nitrotyrosine 10) at pH 6.45 with various metals. The resonance labeled NT-10 is due to the H-2 resonance of nitrotyrosine 10. Concentrations and spectral acquisition parameters are as in Figure 1.

(Elberfeld, Germany). Low molecular weight impurities were removed by ultrafiltration at room temperature using Amicon cells (25- and 43-mm sizes) with Diaflo UM2 membranes in 30 mM ammonium bicarbonate buffer, pH 7.8 to 8.0. The protein solution was frozen at −25 to −30 °C and lyophilized. Pipes was from Calbiochem. D_2O was obtained from Bio-Rad; DCl and NaOD were from Stohler Isotope Chemicals. Lanthanide metals were purchased as the oxides from Johnson-Matthey and were Specpure grade. Sephadex G-25, G-50, and CM-25 were from Pharmacia Fine Chemicals. All other materials were reagent grade.

Mono- and dinitrated BPTI derivatives were prepared as described previously (Snyder et al., 1975). Protein solutions used in the NMR experiments were 2.4 to 2.5 mM BPTI in D_2O buffer containing 15 mM Pipes, 0.1 M KCl, and about 0.5 mM DSS. pH was adjusted by addition of diluted DCl or NaOD in D_2O and was measured with an Ingold 14203 electrode using a Beckman Expandomatic SS-2 or Corning Model 112 pH meter. All pH values reported are uncorrected meter readings. Lanthanide metals were added by addition of the appropriate amount of the stock solution with a 10-μl Hamilton syringe.

^{1}H NMR spectra were obtained at 250 MHz on the MPC-HF 250-MHz superconducting spectrometer (Dadok et al., 1970) using correlation spectroscopy (Dadok and Sprecher, 1974). The spectrometer was locked on the residual HDO peak, except for the Gd(III) experiments, where an external capillary of HMDS was used. The frequency of internal DSS was measured for each sample using 15 to 25 scans of the region upfield of HDO. Chemical shifts reported are relative to DSS, but the reported spectra were aligned on the upfield doublet of tyrosine 23, which did not show any lanthanide induced shifts, or shifts with pH, and therefore was used as an internal standard for the aromatic region. Due to inherent line width, and some spectrometer drift, chemical shifts are no better than ±0.01 ppm. The 270-MHz ^{1}H NMR spectra were obtained on a Bruker HX-270 superconducting spectrometer (90° pulse = 9 μs). At least 1024 transients were collected (8K data points) and Fourier transformed, using pulsed homonuclear irradiation to suppress the residual HDO resonance. Chemical shifts were measured relative to internal DSS and are ±0.01 ppm.

Pr(III) and Eu(III) Experiments

The region of the spectrum downfield of HDO is considered below since it contains many more resolved resonances than the aliphatic region upfield of HDO, and because numerous earlier reports on the aromatic region facilitate the understanding of the lanthanide experiments. Resonances have been attributed to types of protons, such as buried backbone NH's phenylalanine rings and α-CH's (Karplus et al., 1973; Masson and Wüthrich, 1973). Moreover, tyrosine and nitrotyrosine resonances have been assigned to positions within particular residues within the molecule (Snyder et al., 1975). The lower trace of Figure 1 shows native BPTI at pH 6.45. The region between 10.7 and 7.9 ppm consists of nine relatively broad resonances of area one which are associated with buried NH protons. The area of the NH 8 resonance[2] at 8.2 ppm varies depending on sample preparation. Presumably it is less buried than the others and hence is more susceptible to exchange with solvent D_2O. The resonance of area two at 7.82 ppm arises from two overlapping resonances, one associated with a buried NH and the other with an area one doublet of tyrosine 35. The region between 7.7 and 6.0 ppm consists of phenylalanine and tyrosine resonances. Specifically, the doublet of area two at 6.37 ppm arises from the 3, 5 protons of tyrosine 23, which are ortho to the hydroxyl group. Finally at 5.7 ppm there is a broad envelope consisting of two overlapping α-hydrogen resonances.

Before lanthanide ions may be used to investigate the structure of a molecule, three necessary controls are to determine the effects of pH, nitration, and the presence of trivalent metal ions. The 270-MHz ^{1}H spectra of native BPTI taken between pH 3.5 and 8.0 showed no significant changes in the region downfield from 5.2 ppm. Since this region encompasses all 36 aromatic protons of the tyrosines and phenylalanines, nine resolved NH's, and at least two α-CH's, this implies a large portion of the structure is insensitive to the state of protonation of BPTI's five carboxyl groups. Similarly, the only changes accompanying mononitration are associated with the tyrosine 10 resonances themselves (Snyder et al., 1975). In contrast, nitration of tyrosine 21 affects some phenylalanine resonances, NH's 4 and 5 and α-CH 1, as seen by comparison of the lower traces in Figures 2 and 3. These latter three resonances titrate with pH in the absence of lanthanides with a log K_a of 6.4 ± 0.1, a value identical with that of nitrotyrosine 21. Therefore, because only a small number of resonances are sensitive to modification at tyrosine 21, differences in lan-

[2] The numbering of the NH (1 through 9) and α-CH (1 and 2) resonances corresponds to the order of appearance in decreasing chemical shift from internal DSS in native BPTI at pH 7. In contrast, tyrosines 10, 21, 23, and 35 are numbered according to their position in the polypeptide sequence. Backbone NH and α-CH positions are in italics.

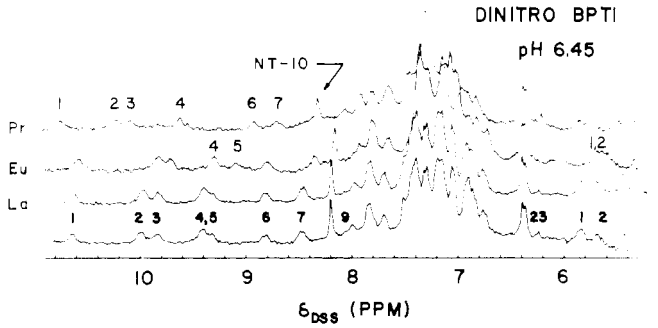

FIGURE 3: Low-field portion of the 250-MHz NMR spectrum of dinitrated BPTI (nitrotyrosines 10 and 21) at pH 6.45 with various metals. Concentrations and spectral acquisition parameters are as in Figure 1.

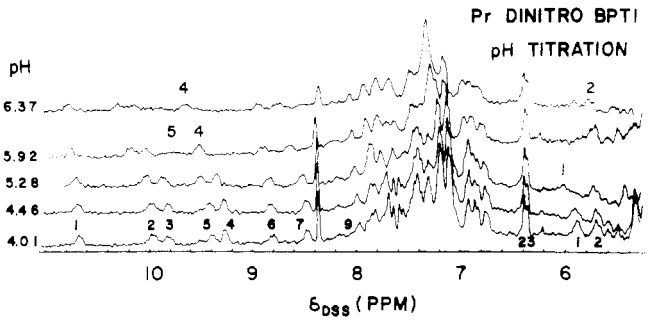

FIGURE 4: Low-field portion of the 250-MHz NMR spectrum of dinitrated BPTI with Pr(III) at various pH's. Concentrations and spectral acquisition parameters are as in Figure 1. Series is obtained by adding small amounts of DCl to the highest pH sample.

thanide induced effects in dinitro- and mononitro-BPTI will be attributed to metal binding at nitrotyrosine 21 rather than to large structural changes. Figures 1, 2, and 3 present the aromatic region of the 250-MHz ^{1}H NMR spectra of native and mononitro- and dinitro-BPTI at the same concentration and pH. Comparison of spectra in the presence and absence of La(III) (the lower two traces of each figure) monitors any changes associated with the introduction of the +3 charge. Due to its $4f^0$ electronic configuration, La(III) is diamagnetic and cannot induce the paramagnetic effects associated with the rest of the lanthanide series (Bleaney, 1972). The identity of the traces indicates the absence of any electrostatic effects under the experimental conditions employed.

Effects due to metal binding at carboxyl side chains, nitrotyrosine 10 and nitrotyrosine 21 can be differentiated by comparison of the spectra of the native and nitrated proteins and by varying the pH of the solution. Figure 4 shows the pH titration of a sample of Pr(III)–dinitro-BPTI. Since the proton stability constants of carboxyl groups are lower than those of nitrotyrosines, the latter binding site can be "turned off" by lowering the pH below the log K_a of nitrotyrosine, while a significant fraction of carboxyl sites will remain available for binding. An interesting feature is that NH's 4 and 5 cross over each other during the pH titration of dinitro-BPTI in the absence of metals, as seen in Table I. They are superimposed at pH 6.1. The determination of the crossover of the two resonances is unambiguous due to their motions in opposite directions. Further, the NH 4 resonance is narrower than the NH 5 resonance throughout the titration, as seen in the lower traces of Figures 3 and 4. Since resonance 4 in native and mononitro-BPTI is narrower than resonance 5, as seen in the lower traces of Figures 1 and 2, the NH 4 resonance in dinitro-BPTI is presumed to arise from the same NH proton associated with resonance 4 in the native inhibitor.

A comparison of Figures 1, 2, and 3 reveals that NH resonances 3 through 7 and α-CH 1 experience Pr(III) and Eu(III) induced paramagnetic shifts only in dinitro-BPTI; hence these shifts may be ascribed to metal bound at nitrotyrosine 21. Their behavior will be used below to derive the stability constant for the binding of lanthanide metals to the nitrotyrosine 21 ring. Paramagnetic shifts observed for the H-2 resonance of nitrotyrosine 10 are due to metal bound at the nitrotyrosine 10 ring with negligible contributions from carboxyl bound metal since there is no Pr(III) induced shift for this resonance at low pH, where only carboxyl sites are capable of metal binding. In addition, the identity of lanthanide induced shifts for this proton in mono- and dinitro-BPTI indicates that nitrotyrosine 21 induced shifts are small. NH resonances 1 and 9 are shifted in native BPTI, are shifted by the same amount in mononitro BPTI, and experience larger shifts in the dinitro derivative. Thus they must be influenced both by carboxyl groups and nitrotyrosine 21. The NH 2 resonance experiences lanthanide induced shifts in mononitro-BPTI and larger shifts in the dinitro derivative, implying interactions with metals bound at both nitrotyrosines 10 and 21.

The quantitative analysis of these experiments is based on the fact that ligands with active protons show alterations in their pH behavior in the presence of metal ions, from which the stability constants of the metal–ligand system may be obtained (Chabarek and Martell, 1959). The fast exchange averaged chemical shift contains contributions from three species where the chelating function is deprotonated, protonated, or bound to metal:

$$\omega_{obsd} = \omega_L P_L + \omega_{HL} P_{HL} + \omega_{ML} P_{ML} \qquad (1)$$

where P_i is the fractional population of species i and ω_i is its chemical shift. As shown in the Appendix, the pH dependence of the chemical shift in the presence of metal ion follows the form of a normal pH titration curve with an apparent proton stability constant

$$K_X = K_a/[1 + K_1'(M_0 - L_0)] \qquad (2)$$

where K_a is the proton stability constant in the absence of metal (Sillen and Martell, 1971), K_1' is the effective metal ligand stability constant, M_0 and L_0 are the total available metal and ligand concentrations, and K_X is the apparent proton stability constant. Hence, the metal–ligand system will titrate at a lower pH than the ligand system alone. The limiting chemical shifts at low and high pH (ω_{HX} and ω_X, respectively) are functions of the shifts of the L, HL, and ML species. The low pH shift is identical with ω_{HL} and the high pH shift is a function of ω_L and ω_{ML}. The constants ω_L and ω_{HL} can be independently measured from the pH dependence of the ligand in the absence of metal and, with these, ω_{ML} may be obtained from ω_X.

The results of nonlinear least-squares fits to the data of Figure 4 are presented in Table I. The fact that the apparent log K_X for NH's 3 through 7 and α-CH 1 is $\geq$5.9, in conjunction with eq 2, implies that the chelator responsible for the shifts must have log $K_a \geq 5.9$, providing further confirmation that these effects arise from nitrotyrosine. Note the observed equality of the low pH limiting shifts measured in the presence (ω_{HX}) and absence (ω_{HL}) of metal ion for NH's 3 through 7 and α-CH 1, a result expected where there is an interaction with one chelating site. These shifts are also apparently equal for NH's 1 and 9, but these are known to interact with both carboxyl and nitrotyrosine bound metal. Table I shows that the apparent proton stability constant (K_X) is lower for NH's 1 and 9 than for NH's 3 through 7 and α-CH 1. This is due to

TABLE I: Parameters from pH Titrations of Dinitro-BPTI.[a]

	NH 1	NH 2	NH 3	NH 4	NH 5	NH 6	NH 7	NH 9	α-CH 1	Av[f]	NO_2 10[l] H-2
Log K_x[b,g]	5.7[h]	6.1	5.9	6.0	5.9	6.0	6.1	5.5[h]	5.9	6.0	6.36
ω_X[b,i]	10.83	10.51	10.30	9.82	10.17	9.01	8.90	8.08	6.62		7.91
ω_{HX}[b,j]	10.67	9.96	9.80	9.26	9.38	8.81	8.46	7.97	5.88		8.35
Log K_a[k]				6.3	6.5				6.5		6.52
ω_{HL}[c,j]	10.66	9.95	9.80	9.27	9.37	8.81	8.46	7.95	5.88		8.37
ω_L[c,j]	10.65	10.02	9.86	9.48	9.31	8.84	8.48	8.05	5.80		8.05
ω_{LaL}[c,i]	10.63	9.98	9.83	9.40	9.32	8.81	8.47	7.98	5.83		8.19
Log K_1(A)[d,h]	2.6	2.0	2.2	2.1	2.2	2.2	2.0	2.8	2.2	2.1	1.7
Log K_1(B)[d,h]	2.6	2.0	2.3	2.1	2.2	2.2	2.0	2.9	2.3	2.2	1.7
Log K_1(C)[d,h]	2.7	2.1	2.3	2.2	2.3	2.3	2.0	2.9	2.3	2.2	1.7
$\omega_{ML} - \omega_{LaL}$(A)[e]			0.7	0.6	1.3[h]	0.3[g]	0.7		1.2[h]		−0.5
$\omega_{ML} - \omega_{LaL}$(B)[e]			0.7	0.6	1.3[h]	0.3[g]	0.7		1.3[h]		−0.5
$\omega_{ML} - \omega_{LaL}$(C)[e]			0.8	0.7	1.4[h]	0.3[g]	0.7		1.3[h]		−0.6

[a] Data from spectra of Figures 3 and 4, as well as a series at 270 MHz at the same protein concentration with no metal present. All stability constants are reported as logarithm and chemical shifts are parts per million from internal DSS. Downfield shifts are *positive*. (A) Assuming carboxyls 30% saturated. (B) Assuming carboxyls 40% saturated. (C) Assuming carboxyls 50% saturated. [b] Nonlinear least-squares fits to data of Figure 4. [c] Observed shifts from Figure 3 and separate titration with no metal. [d] Stability constant for Pr(III) binding to nitrotyrosine 21, calculated from eq 2, for various conditions. [e] Pr(III) induced bound shift, relative to diamagnetic La(III). Calculated from eq A5 for various conditions using averaged stability constant (±0.2 unless otherwise noted). NO_2 10 H-2 data is for Eu(III). [f] Average of data from NH's 3–7 and α-CH 1. [g] ± 0.1. [h] ± 0.3. [i] ± 0.05. [j] ± 0.02. [k] Observed proton stability constant ± 0.1. [l] Data from a Eu(III)–mononitro-BPTI pH titration at 270 MHz, analogous to Figure 4.

the influence of carboxyl side chains, which are contributing to the shifts observed for the former two protons. The net observed shift thus contains a component titrating at low pH and, when the data are fit to a single titration curve, the fitted proton stability constant will be lower than for the NH's affected by nitrotyrosine alone. The data for NH's 3 through 7 and α-CH 1 were combined to obtain an average log K_1' for nitrotyrosine 21. It can be seen that both the derived log K_1' value and the calculated paramagnetic bound shift ($\omega_{ML} - \omega_{LaL}$) are relatively insensitive to assumptions about the metal and proton stability constants for carboxyl groups. The detailed interpretation of the lanthanide induced shifts will be considered in a subsequent manuscript.

In BPTI, there are several different chelating sites possible. To calculate equilibrium concentrations of metal-bound species, full multiple equilibrium calculations were performed using literature values for the proton and metal ion stability constants for carboxyl groups (Sillen and Martell, 1971; Mahler and Cordes, 1966) and nitrotyrosines (Snyder et al., 1975; Marinetti et al., 1975). The results of the calculation were used to correct the value of M_0 used in eq 2 and log K_1' values were calculated for metal binding to nitrotyrosine. Another iteration was performed using the new log K_1' to refine the fraction of metal bound to carboxyl groups. The value of log K_1' for nitrotyrosine 21 (2.2) was taken from the NH 3 through 7 and α-CH 1 data since they were seen to be affected by this chelator alone. The value for nitrotyrosine 10 (1.7) is from analysis of a separate 270-MHz pH titration of a Eu(III)–mononitro-BPTI sample in which the resolved H-2 resonance of the nitrotyrosine 10 ring was monitored.

Gd(III) Experiments

In comparing the shifts of various protons induced by Pr(III) and Eu(III), the correlation between the magnitude of the shift and the distance between the protons and the metal is complicated by a dependence on angular factors as well as distance (Bleaney, 1972). To get direct distance information, experiments were conducted with Gd(III), which is a relaxation probe. The Gd(III) ion has a $4f^7$ configuration and cannot induce dipolar shifts like Pr(III) and Eu(III) (Bleaney, 1972). It can have a scalar interaction with nuclei in the paramagnetic complex, which is transmitted through chemical bounds (Bloembergen, 1957a,b; LaMar et al., 1973). Results on a nitrotyrosine model compound (Marinetti et al., 1975) indicated that these types of interactions were small compared with the dipolar interaction, even for the ring protons and, hence, will certainly be neglibible for other NH, α-CH, and aromatic protons which are removed by several or many more bonds. Gd(III)-induced relaxation will be significant only for protons in close proximity to the metal because of the inverse sixth power dependence on distance of the dipolar relaxation mechanism.

Figure 5 shows a Gd(III) titration with dinitro-BPTI with a large excess of La(III) present to buffer the concentrations of metal-bound species, and to minimize spurious effects, such as metal binding to the glass of the NMR tube (Jones et al., 1974), which could become significant at low concentrations of Gd(III). Similar experiments were performed with native and mononitro-BPTI, and the observed slopes of line width vs. Gd(III) concentration are given in Table II. There are several resonances which show a preponderant contribution from one particular metal binding site. NH's 3, 4, 5, 6, and 7 all show sharp increases in slope in the dinitro derivative as compared with native or mononitro-BPTI, and hence the bulk of the relaxation must be due to metal bound at nitrotyrosine 21. Similarly, NH 2 shows most of its slope increase in mononitro-BPTI, and the excess over native BPTI can be ascribed to nitrotyrosine 10. NH's 1 and 9 show significant line broadening in native BPTI and NH 1 has further increase in dinitro-BPTI. Due to the lack of any increase in slope from native to mono- and dinitro-BPTI, tyrosine 23 appears only to be affected by carboxyl-bound metal, and the interaction is weak. These observations correlate well with the Pr(III) and Eu(III) shifts observed above.

A singular case is that of the H-2 resonance of nitrotyrosine 10, which shows a decrease in slope between mono- and dini-

TABLE II: Gd(III) Line-Broadening Data.

Resonance	Slope of $\Delta\nu$ vs. mM Gd(III) in Hz/mM			Distances[e] of Obsd Protons to Chelating Sites of Dinitro-BPTI		
	Native[a]	Mononitro[a]	Dinitro[a]	Nitrotyrosine 10	Nitrotyrosine 21	Effective Carboxyl
NH 1	10	11	25	>8	9.9	9.7
NH 2	3	15	19	6.5	>12	>11
NH 3	1	1	12	>8	10.4	>11
NH 4	3	5	29	>8	9.0	>11
NH 5	9	4	26	>8	9.4	10.3
NH 6	3	3	20	>8	9.6	>11
NH 7	7	4	12	>8	11.5	>10
NH 9	21	24[b]	16[b]	>8	>12	8.5
Tyr 23	6[c]	5[c]	5[c]	>8	>12	10.7
NO_2 10 H-2		31	10		>12	
α-CH 1	} 5	} 8	40[d]	>8	8.7	>11
α-CH-2			7	>8	>12	>11

[a] Slope of $\Delta\nu$ vs. mM Gd(III) in Hz/mM for specific experimental conditions listed in the legend to Figure 5; ±4 unless otherwise stated. [b] ± 6. [c] ± 2. [d] ± 9. [e] Distances in Å; ±15% or less.

tro-BPTI. One explanation is that NH 8, which occurs at the same chemical shift as nitrotyrosine 10 H-2, is not completely exchanged away in mononitro- but gone in dinitro-BPTI, and adds a broad intensity to the baseline under the nitrotyrosine peak. This would cause the line width of the nitrotyrosine peak to be overestimated, particularly for the spectra with more Gd(III), where the resonance is broadened. The small chemical shift seen in Figure 5 between traces A and B is due to a slight pH change which occurred in the time between recording the spectra of Figures 1 through 3 (including spectrum in Figure 5A) and the upper traces of Figure 5. It is not observed in the behavior of the nitrotyrosine 10 H-2 resonance in mononitro-BPTI, and cannot be ascribed to Gd(III).

The increase in line width for a given nucleus due to Gd(III) bound at site i will be proportional to terms of the form (Swift and Connick, 1962; Dwek, 1972)

$$\Delta\nu_i = 1/[\pi(T_{2i} + \tau_{Mi})] \quad (3)$$

where T_{2i} is defined by

$$\frac{1}{T_{2i}} = \frac{\gamma_I^2 g^2 \beta^2 J(J+1)}{15 r_i^6} \times \left[4\tau_{ci} + \frac{3\tau_{ci}}{1 + \omega_I^2 \tau_{ci}^2} + \frac{13\tau_{ci}}{1 + \omega_S^2 \tau_{ci}^2} \right] \quad (4)$$

In eq 4, γ_I is the gyromagnetic ratio of the proton, g is the electronic g factor, β is the Bohr magneton, J is the spin angular momentum of the Gd(III) ion ($J = 7/2$), r_i is the distance of the proton to the metal in site i, τ_{ci} is the correlation time of the dipolar interaction, ω_I and ω_S are the proton and electron Larmor frequencies, respectively, in radians per second, and τ_{Mi} is the lifetime of the metal bound at site i. For future reference, the quantity in brackets will be denoted $f(\omega, \tau_c)$ and the constant factor in front takes the value 2.583×10^{17} s^{-2} Å^6.

The use of this expression involves several simplifications: (1) Scalar $A\mathbf{I}\cdot\mathbf{J}$ interactions are neglected. This is quite reasonable, as discussed above. (2) $\omega_S \gg \omega_I$; this is always true since the electronic magnetic moment is 654 times larger than that of the proton. (3) The interaction is characterized by a single correlation time, τ_{ci}, which is defined as $1/\tau_{ci} = 1/\tau_{Mi} + 1/\tau_R + 1/\tau_{Si}$, where these times are the bound lifetime of the metal, the rotational correlation times of the Gd(III)-BPTI complex, and the electron spin relaxation time, respectively, for site i. Molecular tumbling is assumed to be isotropic, only a single electron spin relaxation time is considered, and the overall τ_{ci} is assumed much shorter than the shortest T_{2i}. If internal motions are present, $f(\omega, \tau_c)$ will be altered (Woessner, 1962; Wallach, 1967) to include terms involving the correlation time for the internal motion, τ_{int}. In general the shortest time will dominate the overall correlation time, and as will be seen τ_{Mi} is at least 100 times longer than τ_R, so τ_{ci} will be determined by τ_R, τ_{int}, and τ_{Si}. To further simplify the treatment, the following assumptions are also made. (4) The carboxyl and nitrotyrosine binding sites all behave independently: metal binding at one site does not affect metal binding at another, beyond the effects due to the fact that all the seven possible binding sites compete for the same supply of available metal. Further all carboxyl sites are assumed equivalent.

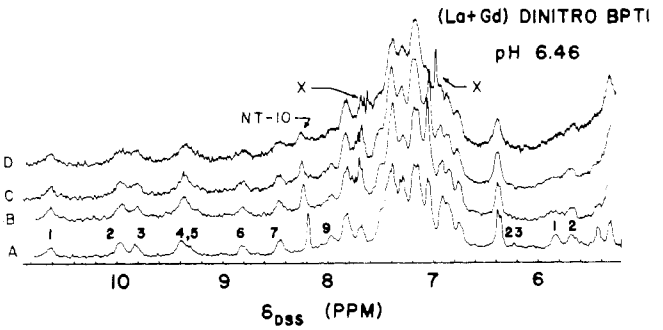

FIGURE 5: Low-field portion of the 250-MHz NMR spectrum of dinitrated BPTI with varying concentrations of Gd(III). Buffer concentrations and spectral acquisition parameters are as in Figure 1. [Protein] = 2.4 mM; [La(III)] = 16.7 to 17.1 mM, pH 6.4. [Gd(III)] for different solutions are as follows: (A) 0 mM; (B) 0.32 mM; (C) 0.63 mM; and (D) 1.09 mM. Series was obtained by adding small amounts of a Gd(III) stock solution of [Gd(III)] = 40 mM and pH 3 to solution A. The resonances labeled X are due to impurities in the HMDS capillary used to lock the spectrometer.

In fast exchange, the observed increases in linewidth for a given resonance will contain contributions from line broadening due to Gd(III) bound at each chelating site, weighted by the fractional population of bound Gd(III). Letting P_i be the fractional population of Gd(III) bound at site i, and denoting the line width in the absence of Gd(III) as $\Delta\nu_0$, one has

$$\Delta\nu_{obsd} = \Delta\nu_0 + \sum_{i=1}^{7} P_i \Delta\nu_i \quad (5)$$

where $\Delta\nu_i$ is the line broadening due to a Gd(III) bound at site i from eq 3. Taking the derivative of this expression with respect to the millimolar concentration of Gd(III), denoted as x, this becomes

$$d\Delta\nu_{obsd}/dx = \sum_{i=1}^{7} (\partial P_i/\partial x)\Delta\nu_i \quad (6)$$

Thus, the contribution of site i to the observed slope is weighted by its derivative of fraction bound with respect to [Gd(III)]. These derivatives are obtained from the calculated values of P_i as a function of [Gd(III)]. These values are 3.3×10^{-2}, 1.1×10^{-2}, and 2.8×10^{-2} mM^{-1} for carboxyl groups, nitrotyrosine 10, and nitrotyrosine 21, respectively.

To calculate distances from line-width data, the correlation time of the Gd(III)-^{1}H interaction must first be estimated. In the case of nitrotyrosine 21, the most obvious method is to use the ring protons to calibrate the interaction since their distance to the metal is known. Unfortunately, they are not sufficiently resolved to permit quantitative analysis of line widths. However, a bound on τ_c may be obtained by examination of Figure 5. At this pH, the H-5 and H-6 resonances of nitrotyrosine 21 ride on top of the upfield Tyr-35 resonances. After the first aliquot of Gd(III) is added, these lines are broadened beyond detection, leaving the Tyr 35 resonances resolved. A lower limit on the line width can be obtained by noting that an area one resonance such as an NH (whose line width is >20 Hz) would be visible, so the line width of nitrotyrosine 21 H-5 and H-6 must be considerably broader, likely >40 Hz. Taking 15 Hz as the line width in the absence of Gd(III), the slope is calculated to be >78 Hz/mM. Using eq 3 and 6, this means $T_2 < 1.14 \times 10^{-4}$ s. The bound will be most significant for the H-6 proton since it is the furthest away (6.8 Å). Inserting this value and the bound on T_2 into eq 4, $f(\omega, \tau_c)$ is calculated to be $>3.35 \times 10^{-9}$ s. For a model involving only isotropic motion, this means $\tau_c > 6 \times 10^{-10}$ s. The rotational correlation time for BPTI is expected to be about 2×10^{-9} s on the basis of its molecular weight using the Stokes–Einstein relation. Any internal motions present will only decrease τ_c from τ_R since the internal rotation correlation time adds to the overall τ_c in reciprocal fashion (Woessner, 1962). Hence τ_c is bounded between 6×10^{-10} and 2×10^{-9} s. An average value of $(1.3 \pm 0.7) \times 10^{-9}$ will be used below, corresponding to $f(\omega, \tau_c) = (6.0 \pm 2.5) \times 10^{-9}$ s.

For metal binding at nitrotyrosine 10, the experimental data for the resolved H-2 resonance can be used to obtain $f(\omega, \tau_c)$. First, the exchange contribution (τ_M) must be estimated. By definition the metal–ligand stability constant K_1 is the ratio between the forward (k_1) and reverse (k_{-1}) rate constants for the ligation reaction, and τ_M is the reciprocal of k_{-1}. According to pressure jump data for aqueous solutions of lanthanide metals and oxalate (Graffeo and Bear, 1968) and murexide (Geier, 1965), both bidentate oxygen ligands, k_1 is independent of the metal ion for the light lanthanides. The forward ligation step is apparently limited by the rate at which water molecules leave the primary coordination sphere. Using these data, and our estimated stability constants, τ_M is calculated to be 1.3×10^{-6} s, giving $T_2 = 1.74 \times 10^{-4}$ s. Using the known distance (6.0 Å) for H-2, $f(\omega, \tau_c)$ is $(1 \pm 0.5) \times 10^{-9}$ s. If motion is isotropic, this corresponds to $\tau_c = (2 \pm 1) \times 10^{-10}$ s, which is considerably shorter than for nitrotyrosine 21. This could arise either from internal motion or a short τ_S shortening the effective τ_c. Since the Gd(III)–H-2 vector is almost colinear with the C_γ–C_β bond, internal rotation about this bond will not significantly affect relaxation (Woessner, 1962). Hence, if internal motion is shortening τ_c, it must be occurring about C_α–C_β bond as well.

For carboxyl interactions, the line broadening at tyrosine 23 will be used for calibration since it is due entirely to carboxyl bound metal, as is evident from Table II. Assuming all carboxyl groups are equivalent, the contribution to the line width is calculated using eq 6. Inserting numerical values, the sum of $\Delta\nu_i$ is found to be 162 Hz. Since the largest $\Delta\nu_i$ is bounded by the sum of all the terms, $\Delta\nu_i < 162$ Hz or $(T_{2i} + \tau_M) > 1.97 \times 10^{-3}$ s. τ_M is evaluated as above to be 2.5×10^{-6} s, which is clearly negligible compared with the smallest T_{2i}. Hence the exchange lifetime terms may be dropped from the $\Delta\nu_i$, reducing the sum to a sum of $1/T_{2i}$. Using eq 3, this can be recasted as a sum of r^{-6}:

$$\sum_{i=1}^{5} \Delta\nu_i = \pi^{-1} \sum_{i=1}^{5} 1/T_{2i} = (2.583 \times 10^{17}/\pi) \cdot f(\omega, \tau_c) \cdot \sum_{i=1}^{5} r_i^{-6} \quad (7)$$

Defining the inverse sixth power sum of the r_i as r_{eff}^{-6}, $f(\omega, \tau_c)$ may be evaluated from the measured value of the left-hand side, and the value of r_{eff} taken from the known x-ray structure of BPTI (10.73 Å). The result is $f(\omega, \tau_c) = 3.0 \times 10^{-9}$ which gives a $\tau_c = 5 \times 10^{-10}$ for isotropic motion. As with nitrotyrosine 10, internal motions of the carboxyl side chains, or a short τ_S could lead to the shortening of τ_c compared with τ_R.

Using the $f(\omega, \tau_c)$ and the exchange lifetimes calculated as above and the observed data, distances from the chelating sites were calculated and are presented in the right half of Table II. Cases where only a lower bound is given are those for which the contribution to the slope was not judged to be significant. Due to the differences in $\partial P_i/\partial x$ and $f(\omega, \tau_c)$ factors, these bounds are different for the three types of binding site. Using a lower limit of significant change of 4 Hz/mM, the bounds are: >11, >8, and >12 Å for carboxyl, nitrotyrosine 10, and nitrotyrosine 21, respectively.

An important feature of the results is the spatial selectivity due to the nature of the r^{-6} dependence. Protons at short distances (<7 Å) will relax so quickly as to be broadened beyond observation, while those further than 12 Å will not be affected significantly. The Gd(III) probe is very sensitive to the immediate proximity of the metal binding site. If a given proton is strongly affected by Gd(III) known to be bound at a specific site, e.g., nitrotyrosine 21, then it is confined to a small region of space near that site, and this puts quite narrow limits on which of the protein protons are consistent with a given resonance.

Using coordinates calculated from the x-ray structure a screening was undertaken to see what backbone proton positions were compatible with the above distance restrictions. A procedure was adopted whereby the various resonances were classed as to whether or not they were affected by Gd(III) bound at the three types of binding sites. Using the minimum observable slope criterion discussed above, the computer searched the x-ray coordinates. The results of the search are as follows.

(1) NH's 1, 3, 4, 5, 6, and 7 and α-CH 1 are compatible with backbone positions *19, 20, 21, 22, 31, 32,* and *33.* That the first four of these should appear is not too surprising in view of their expected proximity to the nitrotyrosine 21 residue. The last three are part of a section of the polypeptide chain which folds up close to the nitrotyrosine 21 region, a fact not obvious from the primary sequence.

(2) NH 2 is compatible with backbone positions *12, 14,* and *39,* a totally different set from the above. This choice is obviously due to the requirement that this resonance be spatially close to nitrotyrosine 10.

(3) NH 9 is compatible with *2, 23, 40, 45, 54, 55,* and *57.* The Gd(III) data for NH 9 indicate that it is reasonably close to carboxyl group and does not allow screening on the basis of distances from either nitrotyrosines, except for a lower bound.

Discussion and Conclusion

In an earlier paper, we proposed nitrotyrosine as a chelator for lanthanide metals in proteins and determined the magnetic parameters of its interactions in a model compound. There are three fundamental questions which arise concerning the applicability of this binding site in a protein: (1) Will the nitrotyrosyl side chain be able to bind metal when incorporated into a macromolecule? (2) Will effects due to metal bound at nitrotyrosine be separable from those due to naturally occurring chelating sites, such as carboxyl groups? (3) What kind of quantitative information can be obtained from the nitrotyrosine–lanthanide probe?

The results here show quite clearly that the answer to the first two questions is yes, as a glance at Figures 1 through 4 will quickly demonstrate. Comparison of effects seen in nitrated and unnitrated derivatives permits the effects due to the nitrotyrosines to be determined by difference. This can be supplemented by pH variations, which, due to the difference in proton stability constants of nitrotyrosine and carboxyl side chains, is a convenient method for separating effects due to the two types of chelators. In addition, quantitative analysis of the pH variation allows determination of the stability constant for metal binding to the chelating site, as was demonstrated for nitrotyrosines 10 and 21.

The quantitative application considered here is the Gd(III) distance experiment. The interaction depends only on the distance between the metal and the nucleus, and hence is considerably simpler than the dipolar shifts induced by Pr(III) and Eu(III), which depend on the distance and two angles. Our results here show that all but one of the nonexchangeable NH's, and a resolved α-CH, are in a spherical shell of radius <12 Å from the metal binding site at nitrotyrosine 21. A subset of these protons, NH's 3 through 7 and α-CH 1, is further localized by the restrictions imposed by the distances from nitrotyrosine 10 and carboxyl side chains. Coupled with the resistance to exchange with solvent D_2O, and the known positions of the tyrosines in the structure, the Gd(III) distances place a rigid core of the protein in the base of the molecule. Hence, different experimental conditions which change the resistance of the resolved NH's to exchange can be directly related to loosening of a *known* portion of the protein. This information should prove useful in the interpretation of thermal or solvent denaturation in terms of the unfolding of the three dimensional structure.

The Gd(III) results were qualitatively compared with the x-ray structure using a space filling model of BPTI to see which of the compatible backbone NH positions looked buried. Positions *19* and *32* seem exposed, *20, 21, 31,* and *33* somewhat buried, and *22* is very buried. The distance calculated for NH *22* to nitrotyrosine 21 is 9.9 Å, which is within experimental error of the distance measured for NH 3, the resonance most resistant to exchange with D_2O. For the set consistent with NH 2, all NH's appeared exposed except for NH *14* which is tucked behind the cystine 14–38 disulfide bridge. Two points concerning distance measurements with Gd(III) merit discussion. It is very selective, due to the r^{-6} dependence, so only nearby nuclei are affected. Since the calculation of a distance therefore involves a sixth root, errors in the observed relaxation and/or $f(\omega, \tau_c)$ factors are strongly suppressed. Even if the cumulative errors in $\Delta\nu$ and τ_c amounted to an *order of magnitude,* the range of derived distances will be of order $10^{1/6}$, giving about a 50% error. In many applications the exact distance may not be important other than the knowledge that a given observed nucleus is in close proximity to the metal, so observation of a line-broadining effect would be sufficient. The work of Campbell et al. (1975) illustrates this case, where paramagnetic difference spectroscopy using lysozyme and Gd(III) was used to assign the indole N-1 proton resonance of Trp-108. Potential ambiguities in distances can arise due to motions of the side chains which chelate the metal ato, and all calculated distances are averages of r^{-6} over the side chain motion. For nitrotyrosine, the most reasonable motions will be 180° flips of the aromatic ring about C_β–C_γ and possibly 120° jumps about C_α–C_β. The latter motion involves large displacements of the whole aromatic ring and may be strongly hindered by neighboring side chains. The space filling model of BPTI reveals that nitrotyrosine 10 appears quite exposed, and both motions are possible. In contrast, nitrotyrosine 21 appears to be much more constrained by nearby residues and in one orientation of the ring, the chelating function may be inaccessible to a metal ion. Motions about C_β–C_γ would appear to be strongly hindered. These observations parallel the Gd(III) correlation times estimated above: if the variations in the effective τ_c are due to internal motions and not τ_S, then nitrotyrosine 10 experiences more motional freedom than nitrotyrosine 21. The model also shows two positive charges (Lys-41 and Arg-39) close to nitrotyrosine 10. Thus, electrostatic effects, as well as steric interactions, may account for the lowered metal ion stability constants of the nitrotyrosines as compared with the model compound.

The biggest advantage of the nitrotyrosine binding site is that it is a known locus on the protein surface. It opens the use of lanthanide shift probes in proteins which do not possess a naturally occurring binding site for metal ions and, further, the intrinsic binding properties do not require that the protein remain in its native conformational state. This means it could be used as a binding site even under denaturing conditions, where a naturally occurring binding site might be destroyed. Steric interactions with other side chains can of course preclude or alter binding, but this will be true of any potential binding site, whether naturally occurring, or produced by chemical modification. It also offers the three ring protons at known position relative to the metal to serve as calibrations for the magnetic interactions. The quantities required for a distance calculation can be determined or at least bounded *without* reference to a crystal structure. This opens the use of the Gd(III) distance probe to proteins lacking characterization by x-ray crystallography.

Another point related to the use of nitrotyrosine as a chelating site is that binding of the lanthanide metal ions is weak enough that the exchange between the metal free in solution and bound to the protein is fast on the NMR timescale. If the binding were very tight, the exchange would become slow relative to the bound shift or relaxation time. Then the observed NMR resonances would not reflect an average of free and bound parameters, and would require the direct observation of the bound peak. Especially in the case of Gd(III), this latter situation would be impossible due to the nherent large line widths of the species with Gd(III) bound. The ability to observe a fast exchange average allows titrations as in Figure 4, where

the amount of paramagnetic metal bound is increased, thus producing variable shifts. This allows resonances to be followed over a range of shifts, and allows one to assign a given peak in the shifted spectrum to a particular resonance in the unshifted spectrum. In slow exchange, the resonances for the free and bound species are separate and one has no prior way of knowing which peak in the shifted spectrum corresponds to a given peak in the unshifted spectrum, making the observation of shifts somewhat useless. In the case of Gd(III) in the slow exchange limit, one would only observe the resonance of the species without Gd(III) bound since the line width of the Gd(III)-bound species would be far too broad to permit observation.

Corollary uses of this binding site would be for experiments with the fluorescent lanthanides such as Tb(III). Again, the knowledge that the metal was bound at specific known locus could be very helpful in interpretation of spectral changes. A second interesting possibility is for protein crystallographers: a lanthanide metal bound at nitrotyrosine would be a strong scattering center; hence it could prove useful as a heavy atom derivative.

Acknowledgments

The authors thank Dr. Robert Rowan III for many helpful discussions and Farbenfabriken Bayer AG for a generous gift of trypsin inhibitor (Trasylol R). One of us (T.D.M.) especially appreciates the hospitality extended to him by Drs. N. and R. Rowan during several trips to Pittsburgh.

Appendix: Metal Ion Stability Constants Derived from the pH Dependence of Observed Chemical Shifts.

Consider a ligand with one chelating function, which includes an ionizable proton, which can exist in two conformational states, Z and Z′. In one of these states, Z′, the chelator is presumed inaccessible to the metal. For this model, see Scheme I. The constraints on the system are: (1) proton stability constant of the ligand, $K_Z = (HZ)/(H)(Z)$; (2) metal ion stability constant, $K_1 = (MZ)/(M)(Z)$; (3) conservation of ligand, $L_0 = (Z) + (Z') + (HZ) + (HZ') + (MZ)$; (4) conservation of metal, $M_0 = (M) + (MZ)$; (5) isomerization constant of unprotonated ligand, $K_p = (Z')/(Z)$; (6) isomerization constant of protonated ligand, $K_p^H = (HZ')/(HZ)$; (7) proton stability constant of the isomerized ligand, $K_Z' = (HZ')/(H)(Z')$. K_Z' is not independent, but is defined by K_Z, K_p, and K_p^H since they are part of a closed cycle.

The pH behavior of this system will be considered for two cases (A and B). (A) Titration in the absence of metal: the observed chemical shift (in fast exchange) will be the average of the shifts of each species, weighted by its fractional population.

$$\omega = \frac{\omega_Z + K_Z(H)\omega_{HZ} + K_p\omega_{Z'} + K_pK_Z(H)\omega_{HZ'}}{1 + K_Z(H) + K_p + K_pK_Z(H)} \quad (A1)$$

This can be recast in the form of a simple titration curve:

$$\omega = (\omega_L + K_a(H)\omega_{HL})/(1 + K_a(H)) \quad (A2)$$

where

$$\omega_L \equiv (\omega_Z + K_p\omega_{Z'})/(1 + K_p) \quad (A3a)$$

$$\omega_{HL} \equiv (\omega_{HZ} + K_p^H\omega_{HZ'})/(1 + K_p^H) \quad (A3b)$$

$$K_a \equiv K_Z(1 + K_p^H)/(1 + K_p) \quad (A3c)$$

Thus the presence of the conformational equilibria will not be seen: the pH dependence of the ligand chemical shift in absence of metal follows a simple titration curve with parameters which are weighted averages of the parameters of the individual conformers. (B) Titration in presence of metal ion:

Scheme I

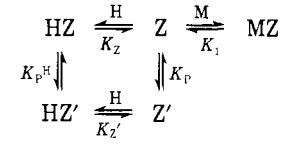

The fast exchange shift is of form

$$\omega = (\omega_X + K_x(H)\omega_{HX})/(1 + K_x(H)) \quad (A4)$$

with

$$\omega_X = \frac{\omega_L + \omega_{ML}[K_1(M_0 - L_0)/(1 + K_p)]}{1 + [K_1(M_0 - L_0)/(1 + K_p)]} \quad (A5a)$$

$$\omega_{HX} = \omega_{HL} \quad (A5b)$$

$$K_x = K_a[1 + K_1(M_0 - L_0)/(1 + K_p)]^{-1} \quad (A5c)$$

where ω_L, ω_{HL}, and K_a are defined by eq A4 and $\omega_{ML} = \omega_{MZ}$.

This has the form of a simple titration curve, but the apparent proton stability constant K_x and the high pH limited shift ω_X are now functions of K_1, M_0, L_0, and K_p. The effect of the conformational equilibria is not observable directly since all that can be determined is $K_1/(1 + K_p)$, which is an effective metal binding constant K_1'.

References

Barry, C. D., Glasel, J. S., North, A. C. T., Williams, R. J. P., and Xavier, A. V. (1972), *Biochim. Biophys. Acta 262,* 101–107.

Barry, C. D., Glasel, J. A., Williams, R. J. P., and Xavier, A. V. (1974a), *J. Mol. Biol. 84,* 471–490.

Barry, C. D., Glasel, J. A., Williams, R. J. P., and Xavier, A. V. (1974b), *J. Mol. Biol. 84,* 491–502.

Bleaney, B. (1972), *J. Magn. Reson. 8,* 91–100.

Bloembergen, N. (1957a), *J. Chem. Phys. 27,* 572–573.

Bloembergen, N. (1957b), *J. Chem. Phys. 27,* 595–596.

Butchard, C. G., Dwek, R. A., Kent, P. W., Williams, R. J. P., and Xavier, A. V. (1972), *Eur. J. Biochem. 27,* 548–553.

Campbell, I. D., Dobson, C. M., and Williams, R. J. P. (1975), *Proc. R. Soc. London, Ser. B 189,* 485–502.

Campbell, I. D., Dobson, C. M., Williams, R. J. P., and Xavier, A. V. (1973), *Ann. N.Y. Acad. Sci. 222,* 163–174.

Chabarek, S., and Martell, A. E. (1959), Organic Sequestering Agents, New York, N.Y., Wiley.

Dadok, J., and Sprecher, R. F. (1974), *J. Magn. Reson. 13,* 243–248.

Dadok, J., Sprecher, R. F., Bothner-By, A. A., and Link, T. (1970), 11th Experimental NMR Conference, Pittsburgh, Pa., Abstracts, section C-2.

Diesenhofer, J., and Steigemann, W. (1974), in Second International Research Conference on Proteinase Inhibitors (Bayer Symposium V), H. Fritz, H. Tschesche, Green, L. J., and Truscheit, E., Ed., New York, N.Y., Springer-Verlag.

Dobson, C. M., Williams, R. J. P., and Xavier, A. V. (1974), *J. Chem. Soc., Dalton Trans.,* 1762–1764.

Dwek, R. A. (1972), *Adv. Mol. Relaxation Processes 4,* 1–53, and reference therein.

Geier, G. (1965), *Ber. Bunsenges. Phys. Chem. 69,* 617–625.

Graffeo, A. J., and Bear, J. L. (1968), *J. Inorg. Nucl. Chem. 30,* 1577–1584.

Huber, R., Kukla, D., Bode, W., Schwager, P., Bartels, K., Diesenhofer, K., and Steigemann, W. (1974), *J. Mol. Biol.*

89, 73-101.
Jones, R., Dwek, R. A., and Forsen, S. (1974), *Eur. J. Biochem. 47,* 271-283.
Karplus, S., Snyder, G. H., and Sykes, B. D. (1973), *Biochemistry 12,* 1323-1329.
LaMar, G. N., Horrocks, W. deW. Jr., and Holm, R. H., Ed. (1973), NMR of Paramagnetic Molecules: Principles and Applications, New York, N.Y., Academic Press.
Mahler, H. R., and Cordes, E. H. (1966), Biological Chemistry, New York, N.Y., Harper & Row.
Marinetti, T. D., Snyder, G. H., and Sykes, B. D. (1975), *J. Am. Chem. Soc. 97,* 6562-6570.
Masson, A., and Wüthrich, K. (1973), *FEBS Lett. 31,* 114-118.
Meloun, B., Fric, I., and Sorm, F. (1968), *Eur. J. Biochem. 4,* 112-117.
Morallee, K. G., Nieboer, E., Rossotti, F. J. C., Williams, R. J. P., Xavier, A. V., and Dwek, R. A. (1970), *J. Chem. Soc., Chem. Commun.,* 1132-1133.
Reuben, J. (1973), *Prog. Nucl. Magn. Reson. Spectrosc. 9,* 1-70.
Reuben, J. (1975), *Naturwissenschaften 62,* 172-178.
Riordan, J. F., and Sokolovsky, M. (1971), *Acc. Chem. Res. 4,* 353-360.
Riordan, J. F., and Vallee, B. L. (1972), *Methods Enzymol. 25,* 515-521.
Sievers, R. E., Ed. (1973), Nuclear Magnetic Resonance Shift Reagents, New York, N.Y., Academic Press.
Sillen, L. G., and Martell, A. E. (1971), Stability Constants of Metal Ion Complexes, London, The Chemical Society.
Snyder, G. H., Rowan, R., III, Karplus, S., and Sykes, B. D. (1975), *Biochemistry 14,* 3765-3777.
Swift, T. J., and Connick, R. E. (1962), *J. Chem. Phys. 37,* 307-320.
Vincent, J. P., Chicheportiche, R., and Lazdunski, M. (1971), *Eur. J. Biochem. 23,* 401-411.
Wallach, D. (1967), *J. Chem. Phys. 47,* 5258-5268.
Woessner, D. E. (1962), *J. Chem. Phys. 36,* 1-4.

Existence of Electrogenic Hydrogen Ion/Sodium Ion Antiport in *Halobacterium halobium* Cell Envelope Vesicles†

Janos K. Lanyi* and Russell E. MacDonald‡

ABSTRACT: Illumination causes the extrusion of protons from *Halobacterium halobium* cell envelope vesicles, as a result of the action of light on bacteriorhodopsin. The protonmotive force developed is coupled to the active transport of Na^+ out of the vesicles. The light-dependent ion fluxes in these vesicles were studied by following changes in the external pH, in the fluorescence of the dye, 3,3′-dipentyloxadicarbocyanine, in the ^{22}Na content of the vesicles, and in [^{3}H]dibenzyldimethylammonium (DDA^+) accumulation. During Na^+ efflux, and dependent on the presence of Na^+ inside the vesicles, the initial light-induced H^+ extrusion is followed by H^+ influx, which results in net alkalinization of the medium at pH > 6.5. When the Na^+ content of the vesicles is depleted, the original net acidification of the medium is restored and large ΔpH develops, accompanied by a decrease in the electrical potential. Data reported elsewhere suggest that the driving force for the transport of some amino acids consists mainly of the electrical potential, while for others it comprises the Na^+ gradient as well. Glutamate transport appears to be energized only by the Na^+ gradient. The development of the Na^+ gradient during illumination thus plays an important role in energy coupling. The results obtained are consistent with the existence of an electrogenic H^+/Na^+ antiport mechanism ($H^+/Na^+ > 1$) in *H. halobium* which facilitates the uphill Na^+ efflux. The light-induced protonmotive force thereby becomes the driving force in forming a Na^+ gradient. The presence of the proposed H^+/Na^+ antiporter explains many of the light-induced pH effects in intact *H. halobium* cells.

The central role of proton translocation across membranes in biological energy transduction has been generally recognized. According to the concept of chemiosmotic energy coupling (Mitchell, 1969, 1970, 1972), the difference in pH and electrical potential between the bulk phases across the membranes constitutes the form in which energy is conserved. The two together give the "protonmotive force", which can drive energy-requiring membrane processes through the movements of H^+ or other ions. One of the energy-requiring processes in bacterial cells is the extrusion of Na^+ against its electrochemical gradient (Zarlengo and Schultz, 1966; Harold et al., 1970; Harold and Papineau, 1972; Lanyi et al., 1976a). In *Streptococcus faecalis* (Harold and Papineau, 1972) and in *Escherichia coli* (West and Mitchell, 1974) the evidence suggests the electrically neutral coupled exchange of Na^+ for H^+ ($H^+/Na^+ = 1$), facilitated by an agent belonging to a class of hypothetical membrane components termed *antiporters* (Mitchell, 1970), similarly to the way the antibiotic monensin is thought to act (Harold, 1970). The extrusion of Na^+ can thus be driven by a pH difference across the membranes (interior alkaline), established either by respiration or ATP[1] hydrolysis.

† From the Biological Adaptation Branch, Ames Research Center, National Aeronautics and Space Administration, Moffett Field, California 94035. *Received March 17, 1976.*

‡ Present address: Section of Biochemistry, Molecular and Cell Biology, Division of Biological Sciences, Cornell University, Ithaca, N.Y. 14850.

[1] Abbreviations used are: DDA^+, dibenzyldimethylammonium ion; TPB^-, tetraphenylboron anion; FCCP, *p*-trifluoromethoxycarbonyl cyanide phenylhydrazone; DCCD, dicyclohexylcarbodiimide; ATP, adenosine triphosphate.